Hindawi Publishing Corporation
Journal of Nanomaterials
Volume 2015, Article ID 374218, 8 pages
http://dx.doi.org/10.1155/2015/374218

Research Article

In Silico Study of Spacer Arm Length Influence on Drug Vectorization by Fullerene C_{60}

Haifa Khemir,[1] Bahoueddine Tangour,[1] and Fathi Moussa[2]

[1]*Research Unity of Modeling in Fundamental Sciences and Didactics, Université de Tunis El Manar, IPEIEM, BP 254, El Manar 2, 2096 Tunis, Tunisia*
[2]*LETIAM, Lip(Sys)[2], University of Paris Sud, IUT d'Orsay, Plateau de Moulon, 91400 Orsay, France*

Correspondence should be addressed to Bahoueddine Tangour; baha.tangour@gmail.com

Received 12 January 2015; Revised 9 May 2015; Accepted 10 May 2015

Academic Editor: Miguel A. Correa-Duarte

This work studies theoretically the effect of spacer arm lengths on the characteristics of a fullerene C_{60}-based nanovector. The spacer arm is constituted of a carbon chain including a variable number of methylene groups ($n = 2$–11). To improve the ability of the fullerene carriage, two arms are presented simultaneously through a malonyl bridge. Then the evolution of selected physicochemical parameters is monitored as a function of the spacer arm length and the angle between the two arms. We show here that while the studied characteristics are almost independent of the spacer arm length or vary monotonically with it, the dipole moment and its orientation vary periodically with the parity of the number of carbon atoms. This periodicity is related to both modules and orientations of dipole moments of the spacer arms. In the field of chemical synthesis, these results highlight the importance of theoretical calculations for the optimization of operating conditions. In the field of drug discovery, they show that theoretical calculations of the chemical properties of a drug candidate can help predict its *in vivo* behaviour, notably its bioavailability and biodistribution, which are known to be tightly dependent of its polarity.

1. Introduction

At the beginning of the 21st century, the fight against cancer remains one of the major public health problems. This is mainly due to some impediments that hinder the achievement of significant therapeutic progress, mainly toxic adverse effects, cell resistance to drugs [1], and high cost of research. A promising way to overcome these obstacles consists in using natural products or some of their extracts. On another hand, drug vectorization and targeting are now recognized as the best way for modulating the bioavailability and thus the toxic adverse effects of an anticancer agent.

Among the different platforms for vectoring active principles (AP) Fullerene C_{60} [2–4] is of particular interest because this carbon nanostructured compound has very interesting biomedical features. Indeed, the toxicity of C_{60} is now well understood [5] and its beneficial health effects encompass a large variety of biomedical fields including imaging, photodynamic therapy, gene delivery [6], oxidative stress [3, 4], and even life extension [7–9].

There are two possible vectorization routes: encapsulation of the AP within the vector or its grafting on the outer walls. The aim of this study is to explore theoretically the vectorization process by grafting thymoquinone (TQ), a model of anticancer natural product, on a fullerene molecule, which is characterized by its nanometric size, high lipophilicity, and chemical reactivity [8].

Thymoquinone (TQ), the most abundant component of black seeds (Nigella sativa), has been used for centuries in the Middle East as a natural medicine for the treatment of many diseases [10, 11]. Several pharmacological studies have demonstrated that TQ is able to develop antioxidant, anti-inflammatory, and antineoplastic effects *in vitro* as well as *in vivo* against various tumor cells [12–15]. Nowadays, TQ has attracted considerable interest and many reports have shown that the inhibitory effects of this compound are specific of cancer cells, including those of breast, prostate, and pancreas cells [14, 16, 17]. A previous report also showed a higher anticancer activity for nanoparticle encapsulated TQ than for free TQ due to improved cellular uptake and bioavailability

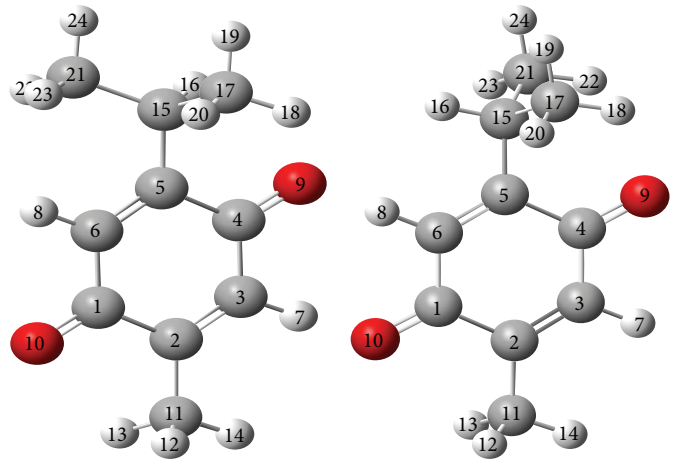

(a) Trans (b) Cis

FIGURE 1: Optimized structures of thymoquinone.

[18], as *in vitro* experiments have shown that the activity of a vectorized drug and the successful operation of vectorization strongly depend on the type of linker used [19–21].

Polarity is an important characteristic of a molecule because it can influence its chemical, physical, and biological properties. Some *in vitro* studies [23] on the activities of a series of histamine H_2 antagonists have shown that relatively minor structural changes greatly influence the antagonistic activity. Because the molecules were very polar, these differences were attributed to the orientations of the dipole moment and interpreted by the relative alignment of hydrogen bonding. For peptides in Aib homooligomers with one, two, and three intramolecular hydrogen bonds, dipole moments increase with the number of Aib units by roughly 2.3 D/residue. The obtained values are 8.22, 10.79, and 12.34 D, respectively [24].

In the research work of Garbuio et al., [25] two series of compounds formed by a nitroxide radical linked by a peptide bond to the fullerene C_{60} are similar to those of our calculated compounds, the authors have shown that the direction of the resulting molecular dipole moment could be changed by reversing the position of fullerene and nitroxide with respect to the nitrogen of the peptide. The electrochemical analysis and chemical nitroxide reduction experiments indicate that the dipole moment significantly affects the redox properties of the two electroactive groups.

Our calculations are designed to study the characteristics and properties of the PA TQ graft on the C_{60} through bra formed by a carbon chain of variable length $-(CH_2)_n$ ($n = 2$–11). This is a relatively inert motif that minimizes interaction with different parts of the human body during drug transport. Its variable length could allow better control of the overall size and physicochemical properties of the studied nanocarriers, which are important parameters for their therapeutic activity.

2. Computational Details

Calculations are computed by the Gaussian [26, 27] packet and recovered by GAUSSVIEW program [28]. Hartree-Fock (HF) and density functional theory (DFT/B3LYP) methods are used for geometrical optimization. Given the great number of atoms forming the studied compound and in order to keep the calculations time compatible with our machines, basis sets STO-3G of moderate dimension were used. For small compounds, the basis set 6-311G(d,p) [29] has also been tested. We checked that all vibrational frequencies are positive, which indicates that each studied structure coincides with a minimum on the potential surface.

3. Results and Discussion

DFT technique has been shown to be reliable and commonly used for the functional study of various nanostructures [30, 31]. The studied compound has a four-part structure consisting of (i) TQ, the active principle, (ii) a spacer arm, (iii) a connecting bridge, and (iv) C_{60} molecule, the drug carrier. To validate our computational techniques and choice of basis sets, we first studied the free TQ molecule. In the second section of this work we focused on the spacer arm and the bridge. The final part deals with the drug candidate that can be synthesized and used in medicine.

3.1. Thymoquinone. Thymoquinone is the 2-isopropyl-5-methyl-1,4-benzoquinone whose molecular formula is $C_{10}H_{12}O_2$ corresponding to two geometrical isomers [32, 33] (Figure 1).

The structure of TQ is optimized in order to enable the localization of any geometrical change induced by its binding to C_{60}. In order to maintain the therapeutic potential of TQ, it is mandatory to avoid any structural modification after its binding to C_{60}.

The calculated values of the geometrical parameters are shown in Table 1. These values are in accordance with those calculated by other authors [22]. Two stable conformations with C1 (trans) and Cs (cis) symmetries (Figure 1) were identified.

Theoretical calculations clearly show that the transconformation is more stable than the cis one. Thus, we continued

Table 1: (a) Geometric parameters values of free and added TQ (trans) onto C_{60}. (b) Theoretical geometric parameters values of free TQ (cis).

(a)

Geometrical parameters	TQ trans							TQ + C_{60}
	STO-3G	6-31G(d)				6-311++G(d,p)		STO-3G
	HF	B3LYP	B3LYP [22]	MPW1PW91 [22]	MP2 [22]	B3LYP [22]	MPW1PW91 [22]	HF
Distances (Å)								
C4–C5	1.503	1.507	1.503	1.497	1.494	1.504	1.497	1.482
C6–C1	1.482	1.481	1.479	1.474	1.475	1.478	1.473	1.503
C1–C2	1.497	1.503	1.498	1.493	1.489	1.498	1.493	1.483
C2=C3	1.336	1.359	1.347	1.343	1.352	1.344	1.340	1.336
C5=C6	1.338	1.361	1.348	1.344	1.354	1.344	1.341	1.338
C4–C3	1.483	1.482	1.479	1.475	1.475	1.479	1.473	1.497
C2–C11	1.505	1.506	1.499	1.491	1.496	1.497	1.489	1.540
C5–C15	1.519	1.520	1.514	1.506	1.505	1.512	1.504	1.540
C15–C17	1.547	1.558	1.546	1.537	1.536	1.545	1.536	1.540
C15–C21	1.537	1.542	1.534	1.525	1.526	1.533	1.524	1.540
C4=O9	1.227	1.261	1.228	1.222	1.240	1.222	1.217	1.227
C1=O10	1.227	1.261	1.227	1.222	1.240	1.222	1.217	—
Angles (°)								
C5–C4–C3	118.9	118.9	118.6	118.7	119.0	118.6	118.6	118.8
C5–C4–O9	121.0	120.8	121.1	120.9	120.9	121.1	121.0	120.4
C3–C4–O9	120.0	120.2	120.3	120.3	120.1	120.3	120.3	120.7

(b)

Geometrical parameters	TQ Cis						
	STO-3G	6-31G(d)				6-311++G(d,p)	
	HF	B3LYP	B3LYP [22]	MPW1PW91 [22]	MP2 [22]	B3LYP [22]	MPW1PW91 [22]
Distances (Å)							
C4–C5	1.502	1.507	1.502	1.497	1.493	1.503	1.496
C6–C1	1.482	1.481	1.479	1.474	1.475	1.478	1.473
C1–C2	1.497	1.503	1.497	1.493	1.488	1.498	1.492
C2=C3	1.336	1.359	1.347	1.343	1.352	1.343	1.340
C5=C6	1.338	1.361	1.349	1.345	1.359	1.346	1.342
C4–C3	1.484	1.483	1.482	1.476	1.477	1.480	1.475
C2–C11	1.505	1.506	1.499	1.491	1.496	1.497	1.489
C5–C15	1.521	1.523	1.517	1.509	1.507	1.516	1.508
C15–C17	1.545	1.553	1.543	1.534	1.533	1.542	1.533
C15–C21	1.545	1.553	1.543	1.534	1.533	1.542	1.533
C4=O9	1.227	1.261	1.228	1.223	1.241	1.222	1.217
C1=O10	1.227	1.261	1.227	1.221	1.239	1.222	1.216
Angles (°)							
C5–C4–C3	118.7	118.7	118.4	118.5	118.7	118.4	118.5
C5–C4–O9	121.7	121.6	121.9	121.8	121.9	121.7	121.7
C3–C4–O9	119.5	119.7	119.7	119.7	119.4	119.8	119.8

the calculations by using the former one. The transisomer is not a very polar compound because its dipole moment is only equal to 0.336 and 0.284 D as calculated with HF/STO-3G and DFT/6-311G(d,p), respectively.

3.2. The Spacer Arm. For the spacer arm, calculations were performed by both HF and DFT. The comparison between the two results was used for results validation in order to compensate the lack of experimental values for these compounds. Each spacer arm is formed by a saturated carbon chain and the number of methylene groups ($-CH_2$) ranged from 2 to 11. At the chain ends, two functions containing OH groups (one primary alcohol and one carboxylic acid) were fixed to be easily substituted by chlorine atoms. The length of the arm is measured between these two fragments (Figure 2). Given the importance of the polarity in the interaction of TQ with the human body [34], a particular attention has been paid to the dipole moment.

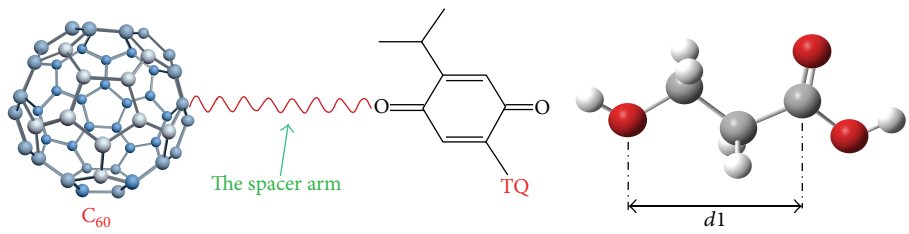

Figure 2: Description of (a) the compound C_{60}-spacer arm-TQ and (b) the spacer arm length ($d1$ (Å)).

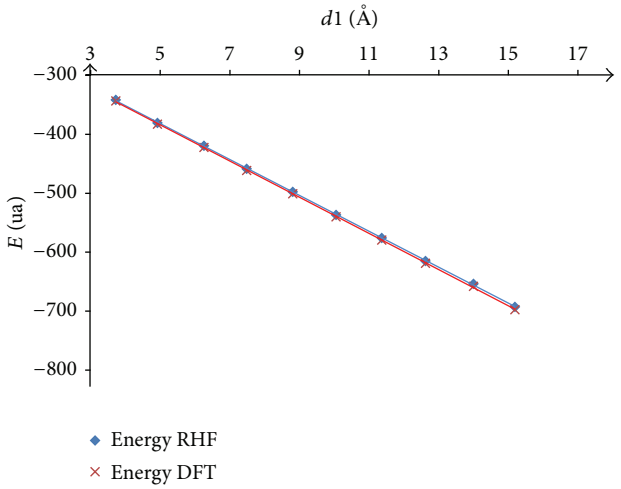

Figure 3: Variation of the optimization energy (E(ua)) HF and DFT versus the length of the spacer arm ($d1$ (Å)).

Table 2: Bond length and dipole moment values of the studied spacer arms.

Compound	Spacer arm length (Å)	Dipole moment (D)	
n	$d1$	HF	DFT
2	3.721	0.42	0.46
3	4.918	3.95	3.52
4	6.254	0.50	0.52
5	7.482	3.93	3.93
6	8.806	0.53	0.53
7	10.05	3.92	3.49
8	11.365	0.55	0.56
9	12.617	3.92	3.47
10	13.998	0.55	0.57
11	15.185	3.92	3.49

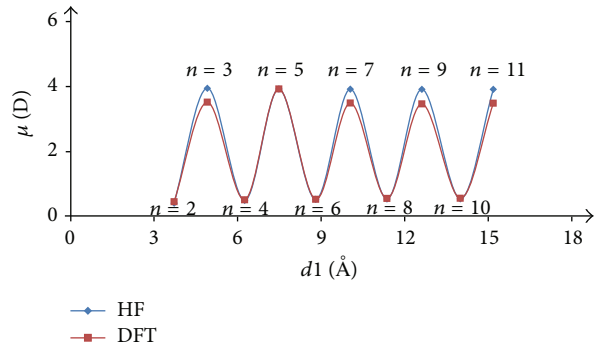

Figure 4: Variation of the dipole moment (μ (D)) versus the spacer length ($d1$ (Å)).

Figure 3 shows the variation of the optimized energy as a function of the spacer arm length. By using HF and DFT methods, we obtained a linear relationship between both parameters ($y = -30.44x - 229.79$ ($R^2 = 0.999$) and $y = -30.67x - 230.93$ ($R^2 = 0.999$), resp.), thus demonstrating that all studied spacer arms have similar behaviour.

In a multistage synthesis process, the yield depends on the correct choice of operating conditions particularly on the choice of the appropriate solvent. For these reasons, a special attention was given to the dipole moments of all studied compounds. Table 2 summarizes the dipole moment values data. These results show large variations as a function of the length of the spacer arm. A periodic phenomenon is observed, with maxima corresponding to even unit numbers of methylene (–CH_2) and minima associated with odd numbers (Figure 4).

The maxima are relatively high, which is consistent with the presence of polar moieties such as carboxylic acids and alcohols. For instance, Furylfulgide (Aberchrome 540) is known to exhibit an experimental dipole moment of 7.2 D [35].

As periodicity is observed, dipole moments values take substantially two different levels depending on the parity of the number of the spacer arm carbon atoms. The figures obtained from the vector shape of dipole moments also show alternating orientation of direction. Each dipole moment is drawn from the electronic barycenter.

To interpret both values and changes in dipole moments, we proceeded step by step. First the arm was divided into three parts, which are alcohol, carboxylic acid, and the remaining CH_2 chain. To take reciprocal fragments interaction into account, we then computed each dipole moment separately with the remaining atoms being replaced by dummy ones as illustrated in Figure 5. So the three calculated dipole moments will have the same representation referential. Hence, we started with the shortest odd number of methylene group ($n = 3$). Given that one CH_2 is included

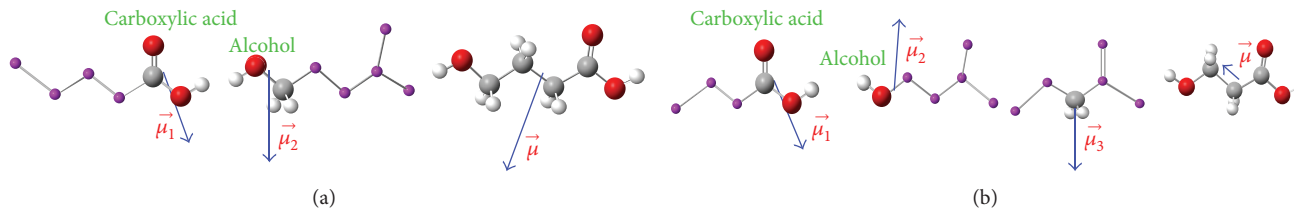

(a) (b)

Figure 5: Dipole moment drawn from the electronic barycenter for the shortest linkers: (a) $n = 3$ and (b) $n = 2$.

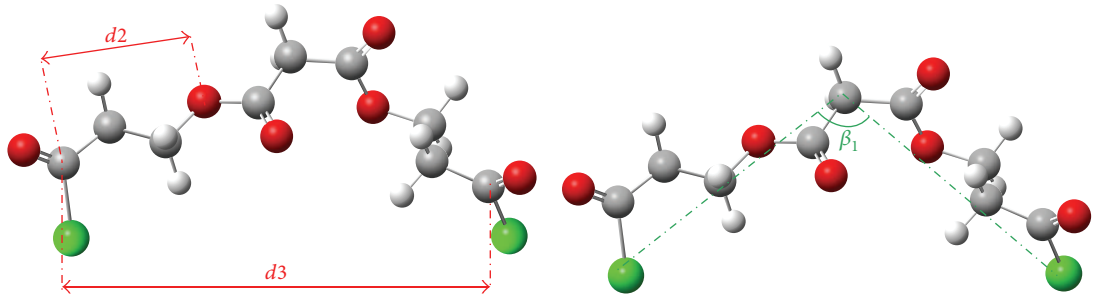

(a) (b)

Figure 6: Descriptors of bridged spacer arms: (a)- ($d2$ (Å)), ($d3$ (Å)) and (b)- ($\beta 1$ (°)). Optimized structures were performed with a chlorine ended atom.

Table 3: Dipole moment values of fragments and their combination.

	Carboxylic acid $\vec{\mu}_1$	Alcohol $\vec{\mu}_2$	CH_2 $\vec{\mu}_3$	$n = 3$ $\vec{\mu}_1 + \vec{\mu}_2$	$n = 2$ $\vec{\mu}_1 - \vec{\mu}_2 + \vec{\mu}_3$
x	1.681	1.26	0	2.941	0.421
y	0.403	−1.99	−2.411	−1.587	−0.018
z	0	0	0	0	0
μ (D)	1.728	2.355	2.411	3.34 3.95[a]	0.42 0.41[a]

[a]DFT calculated value for the studied compound.

in the alcohol function, the remaining carbon motif $-CH_2-CH_2-$ is apolar by symmetry. Adding dipole moments of fragments leads to 3.34 D, which is very close to the DFT calculated value of 3.95 D.

Details of calculations are summarized in Table 3. Roughly the same dipole moment value is obtained for all similar compounds with odd number of methylene groups. This is due to the fact that the central motif is not involved in the final dipole moment, as its partial moment is equal to zero. Moving now to the shortest arm that contains only a single methylene group, a carboxylic acid, and an alcoholic function. Here, the CH_2 group alone becomes polar. Its dipole moment is 2.41 D. One of the other two moments will necessarily change in direction compared to the previous case with odd n. The vector sum of three contributions changes in direction and value. So we get a value of 0.42 D, again close to the DFT calculated one of 0.41 D. A similar reasoning can be extended to all compounds with an even number of CH_2 groups. To summarize these observations, whenever a methylene group is added to the chain, one of the two ended polar fragment moments changes in direction. Thus, the addition and the subtraction of their dipole moment will be alternated.

Given that the DFT technique provides consistent results with those obtained by the HF method results, the latter was chosen for the rest of the calculations as it requires much less computing time. When the number of studied atom patterns is large, theoretical calculations are performed to determine the optimized structures with the different spacer arms attached to C_{60} on three levels: small ($n = 2$), medium ($n = 5$), and large ($n = 11$). In order to increase the efficiency of the proposed protocol, two spacer arms are grafted on a support to connect them simultaneously to the fullerene molecule. The condensation of each spacer arm with malonyl dichloride allows reaching a stable adduct. Hydroxyl groups of the carboxylic end are substituted by chlorine atoms in order to prepare the final compound for the following step of condensation on TQ. Figure 6 depicts the descriptors $d2$ and $d3$ and the $\beta 1$ angle.

The dipole moment of the diagram (Figure 7) is a function of the chlorinated compound length. There is a periodicity of dipole moment as a function of the spacer arm length. However, an inversion of the dipole moment is observed with respect to the arm alone. The highest values are obtained for odd numbers while the lowest values are linked to even ones. The HF results of the descriptors $d2$, $d3$, μ and $\beta 1$ for the chlorinated arms are summarized in Table 4.

3.3. The Final Compound [Arm-TQ]. Theoretical HF calculations were performed to determine the optimized structures of the various compounds of arm spacer's condensation, along with different lengths, with TQ (Figure 8).

Table 4: HF results for the chlorinated spacer arms.

n	$d2$ (Å)	$d3$ (Å)	μ (D)	$\beta1$ (°)
2	3.736	10.293	5.37	119.21
3	4.974	12.143	3.85	119.33
4	6.254	14.583	5.58	119.96
5	7.538	16.567	3.94	120.03
6	8.853	18.941	5.63	119.91
7	10.105	21.011	3.97	120.25
8	11.414	23.371	5.66	120.27
9	12.677	25.453	4.00	120.20
10	13.977	27.783	5.66	120.23
11	15.245	29.891	4.02	120.19

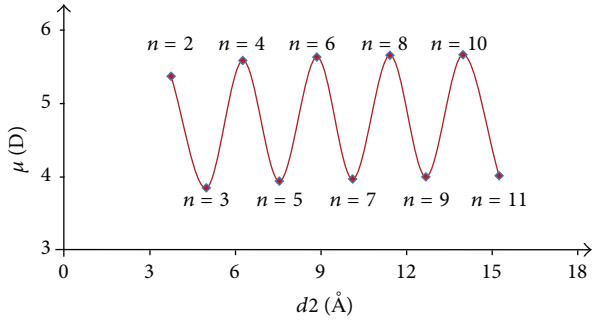

Figure 7: Dipole moment (μ (D)) values versus the length ($d2$ (Å)) of the bridged and chlorinated linker.

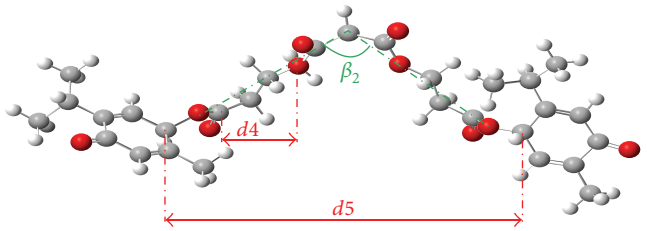

Figure 8: The distances ($d4$ (Å)), ($d5$ (Å)), and ($\beta2$ (°)) of the compound arm and TQ.

Table 5: Characteristics of studied compounds [arm-TQ].

Compounds n	$d4$ (Å)	$d5$ (Å)	μ (D)	$\beta2$ (°)
2	3.74351	13.25676	11.65	101.55929
5	7.48692	17.67825	6.48	90.22772
11	14.91388	32.09813	7.98	80.76277

The relationship between the distance and the angle of the arm shown in Figure 9 obeys the following equation (Table 5): $y = -1.778x + 106.3$ ($R^2 = 0.943$).

The angle of the two support arms decreases when the distance from the spacer arm increases.

3.4. Grafting the Final Compound [Arm-TQ] on C_{60}. The effect of grafting on TQ structure and the experimental geometric parameters for the free TQ grafted onto fullerene

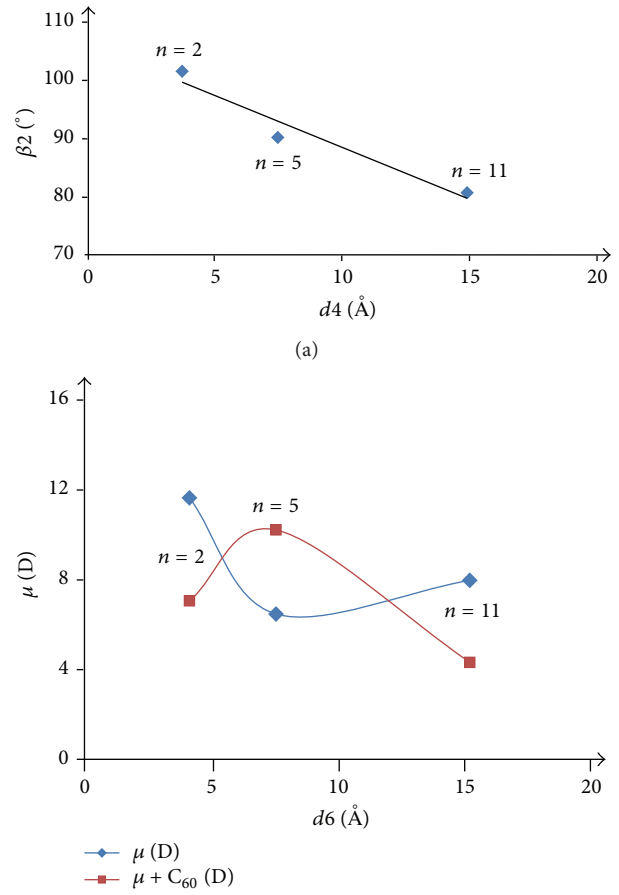

Figure 9: (a) Variation of the angle of opening ($\beta2$ (°)) of compound [arm-TQ] as a function of the distance of the spacer arm ($d4$ (Å)). (b) Variation of the dipole moment (μ (D)) as a function of the length of the spacer arm ($d6$ (Å)) of the compound [Spacer arm-TQ-C_{60}].

Table 6: Descriptors $d6$ and $d7$ and dipole moment of compound arm TQ-C_{60}.

Compounds	$d6$ (Å)	$d7$ (Å)	μ (D)
$n = 2$	4.04684	13.95476	7.0695
$n = 5$	7.48692	17.71344	10.2224
$n = 11$	15.20008	27.16047	4.3283

C_{60} are summarized in Table 1(b). Small changes, in the 1% range, are observed. This demonstrates the conservation of the original structure of TQ thus meeting the first requirement of the vectorization process. Figure 10 shows the final compound corresponding to TQ grafted onto C_{60} via a spacer arm and its descriptors $d6$ and $d7$ (Table 6).

4. Conclusion

In this paper, we studied the effects of the spacer arm length on the synthesis conditions of a fullerene C_{60}-based drug-vector. As a drug sample, we selected thymoquinone, a natural product with anticancer properties. The spacer arm

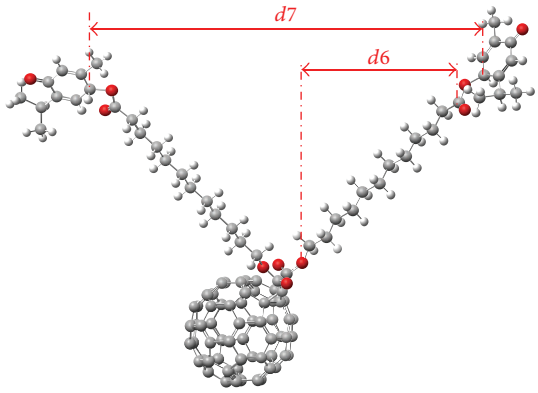

Figure 10: Structure of the final compound [Arm-TQ-C_{60}] and its descriptors ($d6$ (Å)) and ($d7$ (Å)).

was chosen for its biocompatibility since it is composed of a carbon chain including a variable number of methylene groups (n = 2–11) ending with alcohol and carboxylic acid functions. To improve the ability of the fullerene carriage, two arms were grafted simultaneously through a malonyl bridge [36].

All parts of the resulting nanosystem were studied separately. Their geometry was optimized and selected physicochemical parameters were calculated. The evolution of these parameters was monitored as a function of the spacer arm length and the angle between the two arms. While all the studied characteristics were almost independent of the spacer arm length or varied monotonically with it, the dipole moment exhibited periodicity depending on the parity of the number of carbon atoms in the chain. All other studied compounds exhibited the same periodic behaviour. This phenomenon is explained by the alternation of vector addition/subtraction when the parity of carbon atoms number was changed.

In the field of chemical synthesis, these results highlight the importance of theoretical calculations for the optimization of operating conditions. Indeed, the knowledge of chemical properties, notably the polarity of synthesised products and intermediates, is mandatory for the right choice of the solvents. In the field of C_{60}-derivatives synthesis, the rule "like dissolves like" remains of high relevance. Indeed, C_{60}'s solubility is known to be very sensitive to the polarity of the solvent. For instance, its solubility in 1-chloro-naphthalene (S = 50 mg·mL^{-1}) is considerably higher than in methanol (S = 0.01 mg·mL^{-1}) [37]. Hence, changes in the parity of the spacer arm will have a great significance in the synthesis of a C_{60} based nanovector.

As the synthesis process requires several steps, we have to find the appropriate solvent for each combination step that means that the solvent polarity should be controlled according to the parity of the spacer arm and the polarity of each synthesis product or synthesis intermediate. Finally, our results show that theoretical calculations of the chemical properties of a drug candidate can help predict its *in vivo* behaviour, notably its bioavailability and biodistribution, which are known to be tightly dependent of its polarity.

Conflict of Interests

The authors declare that there is no conflict of interests regarding to the publication of this paper.

References

[1] J. Davies, "Inactivation of antibiotics and the dissemination of resistance genes," *Science*, vol. 264, no. 5157, pp. 375–382, 1994.

[2] H. W. Kroto, J. R. Heath, S. C. O'Brien, R. F. Curl, and R. E. Smalley, "C_{60}: buckminsterfullerene," *Nature*, vol. 318, no. 6042, pp. 162–163, 1985.

[3] A. W. Jensen, S. R. Wilson, and D. I. Schuster, "Biological applications of fullerenes," *Bioorganic and Medicinal Chemistry*, vol. 4, no. 6, pp. 767–779, 1996.

[4] H. Szwarc and F. Moussa, "[60] Fullerene and derivatives in biology and medicine," in *Handbook of Fullerene: Synthesis, Properties and Applications*, R. F. Verner and C. Benvegn, Eds., pp. 403–420, Nova Science Publishers, New York, NY, USA, 2012.

[5] J. Kolosnjaj, H. Szwarc, and F. Moussa, "Toxicity studies of fullerenes and derivatives," *Advances in Experimental Medicine and Biology*, vol. 620, pp. 168–180, 2007.

[6] R. Maeda-Mamiya, E. Noiri, H. Isobe et al., "In vivo gene delivery by cationic tetraamino fullerene," *Proceedings of the National Academy of Sciences of the United States of America*, vol. 107, no. 12, pp. 5339–5344, 2010.

[7] K. L. Quick, S. S. Ali, R. Arch, C. Xiong, D. Wozniak, and L. L. Dugan, "A carboxyfullerene SOD mimetic improves cognition and extends the lifespan of mice," *Neurobiology of Aging*, vol. 29, no. 1, pp. 117–128, 2008.

[8] J. Gao, Y. Wang, K. M. Folta et al., "Polyhydroxy fullerenes (fullerols or fullerenols): beneficial effects on growth and lifespan in diverse biological models," *PLoS ONE*, vol. 6, no. 5, Article ID e19976, 2011.

[9] T. Baati, F. Bourasset, N. Gharbi et al., "The prolongation of the lifespan of rats by repeated oral administration of [60]fullerene," *Biomaterials*, vol. 33, no. 19, pp. 4936–4946, 2012.

[10] M. S. Butt and M. T. Sultan, "Nigella sativa: reduces the risk of various maladies," *Critical Reviews in Food Science and Nutrition*, vol. 50, no. 7, pp. 654–665, 2010.

[11] N. Ilaiyaraja and F. Khanum, "*Nigella sativa* L.: a review of therapeutic application," *Journal of Herbal Medicine and Toxicology*, vol. 4, pp. 1–8, 2010.

[12] S. Padhye, S. Banerjee, A. Ahmad, R. Mohammad, and F. H. Sarkar, "From here to eternity—the secret of Pharaohs: therapeutic potential of black cumin seeds and beyond," *Cancer Therapy*, vol. 6, no. b, pp. 495–510, 2008.

[13] C. C. Woo, A. P. Kumar, G. Sethi, and K. H. B. Tan, "Thymoquinone: potential cure for inflammatory disorders and cancer," *Biochemical Pharmacology*, vol. 83, no. 4, pp. 443–451, 2012.

[14] M. N. Nagi and M. A. Mansour, "Protective effect of thymoquinone against doxorubicin-induced cardiotoxicity in rats: a possible mechanism of protection," *Pharmacological Research*, vol. 41, no. 3, pp. 283–289, 2000.

[15] O. A. Al-Shabanah, O. A. Badary, M. N. Nagi, N. M. Al-Gharably, A. C. Al-Rikabi, and A. M. Al-Bekairi, "Thymoquinone protects against doxorubicin-induced cardiotoxicity without compromising its antitumor activity," *Journal of Experimental and Clinical Cancer Research*, vol. 17, no. 2, pp. 193–198, 1998.

[16] A. E. Edris, "Anti-cancer properties of *Nigella* spp. essential oils and their major constituents, thymoquinone and β-elemene," *Current Clinical Pharmacology*, vol. 4, no. 1, pp. 43–46, 2009.

[17] R. Keyhanmanesh, M. H. Boskabady, S. Khamneh, and Y. Doostar, "Effect of thymoquinone on the lung pathology and cytokine levels of ovalbumin-sensitized guinea pigs," *Pharmacological Reports*, vol. 62, no. 5, pp. 910–916, 2010.

[18] J. Ravindran, H. B. Nair, B. Sung, S. Prasad, R. R. Tekmal, and B. B. Aggarwal, "Thymoquinone poly (lactide-co-glycolide) nanoparticles exhibit enhanced anti-proliferative, anti-inflammatory, and chemosensitization potential," *Biochemical Pharmacology*, vol. 79, no. 11, pp. 1640–1647, 2010.

[19] S. Kiyonaka, K. Sada, I. Yoshimura, S. Shinkai, N. Kato, and I. Hamachi, "Semi-wet peptide/protein array using supramolecular hydrogel," *Nature Materials*, vol. 3, no. 1, pp. 58–64, 2004.

[20] S. J. Lee and S. Y. Lee, "Microarrays of peptides elevated on the protein layer for efficient protein kinase assay," *Analytical Biochemistry*, vol. 330, no. 2, pp. 311–316, 2004.

[21] G. J. Wegner, H. J. Lee, and R. M. Corn, "Characterization and optimization of peptide arrays for the study of epitope-antibody interactions using surface plasmon resonance imaging," *Analytical Chemistry*, vol. 74, no. 20, pp. 5161–5168, 2002.

[22] A. B. Raschi, E. Romano, A. M. Benavente, A. B. Altabef, and M. E. Tuttolomondo, "Structural and vibrational analysis of thymoquinone," *Spectrochimica Acta—Part A: Molecular and Biomolecular Spectroscopy*, vol. 77, no. 2, pp. 497–505, 2010.

[23] R. C. Young, G. J. Durant, J. C. Emmett et al., "Dipole moment in relation to H_2 receptor histamine antagonist activity for cimetidine analogues," *The Journal of Medicinal Chemistry*, vol. 29, no. 1, pp. 44–49, 1986.

[24] A. H. Holm, M. Ceccato, R. L. Donkers, L. Fabris, G. Pace, and F. Maran, "Effect of peptide ligand dipole moments on the redox potentials of Au 38 and Au140 nanoparticles," *Langmuir*, vol. 22, no. 25, pp. 10584–10589, 2006.

[25] L. Garbuio, S. Antonello, I. Guryanov et al., "Effect of orientation of the peptide-bridge dipole moment on the properties of fullerene-peptide-radical systems," *Journal of the American Chemical Society*, vol. 134, no. 25, pp. 10628–10637, 2012.

[26] M. J. Frisch, G. W. Trucks, H. B. Schlegel et al., *Gaussian 03, Revision C. 02*, Gaussian, Wallingford, Conn, USA, 2004.

[27] M. J. Frisch, G. W. Trucks, H. B. Schlegel et al., *Gaussian 09 Revision A.1*, Gaussian, Wallingford, Conn, USA, 2009.

[28] A. Frisch, A. B. Nielsen, and A. J. Holder, *GAUSSIANVIEW Users Manual*, Gaussian, Pittsburgh, Pa, USA, 2000.

[29] R. Ditchfield, W. J. Hehre, and J. A. Pople, "Self-consistent molecular orbital methods. 9. Extended Gaussian-type basis for molecular-orbital studies of organic molecules," *The Journal of Chemical Physics*, vol. 54, no. 2, pp. 724–728, 1971.

[30] A. Ahmadi, N. L. Hadipour, M. Kamfiroozi, and Z. Bagheri, "Theoretical study of aluminum nitride nanotubes for chemical sensing of formaldehyde," *Sensors and Actuators B: Chemical*, vol. 161, no. 1, pp. 1025–1029, 2012.

[31] A. Ahmadi, J. Beheshtian, and N. L. Hadipour, "Chemisorption of NH3 at the open ends of boron nitride nanotubes: a DFT study," *Structural Chemistry*, vol. 22, no. 1, pp. 183–188, 2011.

[32] P. J. Houghton, R. Zarka, B. de las Heras, and J. R. S. Hoult, "Fixed oil of *Nigella sativa* and derived thymoquinone inhibit eicosanoid generation in leukocytes and membrane lipid peroxidation," *Planta Medica*, vol. 61, no. 1, pp. 33–36, 1995.

[33] N. Chakravarty, "Inhibition of histamine release from mast cells by nigellone," *Annals of Allergy*, vol. 70, no. 3, pp. 237–242, 1993.

[34] O. A. Badary, O. A. Al-Shabanah, M. N. Nagi, A. C. Al-Rikabi, and M. M. A. Elmazar, "Inhibition of benzo(a)pyrene-induced forestomach carcinogenesis in mice by thymoquinone," *European Journal of Cancer Prevention*, vol. 8, no. 5, pp. 435–440, 1999.

[35] J. A. Delaire and K. Nakatani, "Linear and nonlinear optical properties of photochromic molecules and materials," *Chemical Reviews*, vol. 100, no. 5, pp. 1817–1845, 2000.

[36] C. Bingel, "Cyclopropanierung von fullerenen," *Chemische Berichte*, vol. 126, no. 8, pp. 1957–1959, 1993.

[37] R. S. Ruoff, D. S. Tse, R. Malhotra, and D. C. Lorents, "Solubility of C60 in a variety of solvents," *The Journal of Physical Chemistry*, vol. 97, no. 13, pp. 3379–3383, 1993.